IEEE Photonics Journal
An IEEE Photonics Society Publication

Open Access

A Comparative Study of Radiation-Tolerant Fiber Optic Sensors for Relative Humidity Monitoring in High-Radiation Environments at CERN

Volume 6, Number 6, December 2014

G. Berruti
M. Consales
A. Borriello
M. Giordano
S. Buontempo
A. Makovec
G. Breglio
P. Petagna
A. Cusano

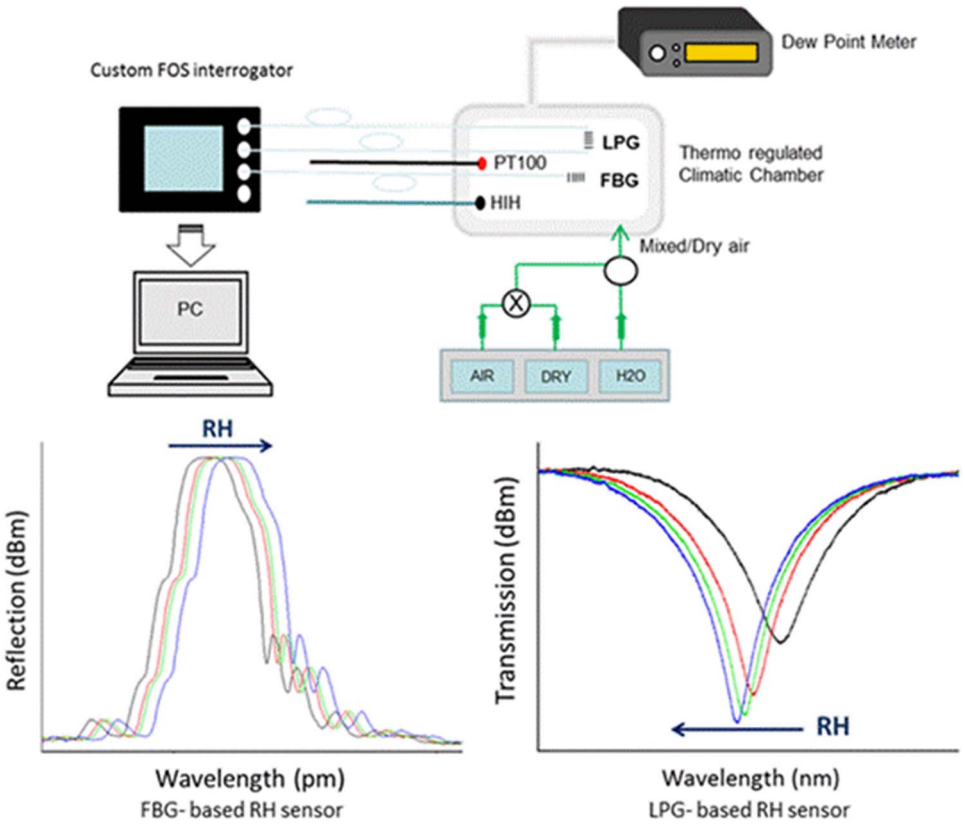

DOI: 10.1109/JPHOT.2014.2357433
1943-0655

A Comparative Study of Radiation-Tolerant Fiber Optic Sensors for Relative Humidity Monitoring in High-Radiation Environments at CERN

G. Berruti,[1,2] M. Consales,[1] A. Borriello,[3] M. Giordano,[3] S. Buontempo,[4] A. Makovec,[5] G. Breglio,[6] P. Petagna,[2] and A. Cusano[1]

[1]Optoelectronics Group, Department of Engineering, University of Sannio, 82100 Benevento, Italy
[2]Physics Department, Detector Technology Section, European Organization for Nuclear Research (CERN), 1211 Genève, Switzerland
[3]Institute for Composite and Biomedical Materials (IMCB), National Research Council, 80055 Portici, Italy
[4]Istituto Nazionale di Fisica Nucleare (INFN), 80126 Napoli, Italy
[5]University of Debrecen, 4032 Debrecen, Hungary
[6]Department of Electrical Engineering and Information Technology, University of Naples "Federico II," 80138 Napoli, Italy

DOI: 10.1109/JPHOT.2014.2357433

Manuscript received June 19, 2014; accepted September 5, 2014. Date of publication September 24, 2014; date of current version December 18, 2014. Corresponding author: Andrea Cusano (a.cusano@unisannio.it).

Abstract: In this paper, we report a comparative study of fiber optic sensors for applications of relative humidity (RH) monitoring in high-radiation environments. In particular, we present investigations carried out since 2011 by our multidisciplinary research group, in collaboration with the European Organization for Nuclear Research (CERN) in Geneva. Our research has been first focused on the development of polyimide-coated fiber Bragg grating (FBG) sensors, and recently, it has been extended to nanoscale metal oxide-coated long-period gratings (LPGs). Experimental tests in the [0–70] %RH range at different temperatures, before and after γ-ionizing radiation exposures, have been carried out to assess the sensors' performances in conditions required in experiments running at CERN. The advantages and disadvantages of the two proposed technologies are discussed in this paper in light of their possible application in high-energy physics environments. In particular, reported results suggest that LPG-based sensors can be preferred in some applications (particularly in presence of very low humidity levels) mainly because they are able to provide very high RH sensitivity (up to 1.4 nm/% RH), which is up to three orders of magnitude higher than that exhibited by FBG-based hygrometers. On the other side, compared with FBGs, LPGs are more difficult to multiplex due to limitations in terms of available bandwidth.

Index Terms: Fiber Bragg grating, long period grating, CERN, relative humidity monitoring, high energy physics.

1. Introduction

The Compact Muon Solenoid (CMS) is one of the two large general-purpose particle physics detectors built on the Large Hadron Collider (LHC) accelerator at the European Organization for Nuclear Research (CERN) in Geneva. The detector is a multi-layered cylinder that is 25 meter

long and 15 meters in diameter, weighing more than 13 000 tons, built around a large solenoid generating a uniform magnetic field of 4 Tesla. Its innermost layer is a silicon-based particle tracker where 16 000 silicon pixel and micro-strip sensors are used to measure momentum and position of the particles emerging from the LHC collisions.

The high radiation dose resulting from the LHC operation at full luminosity can cause loss of performance of the silicon sensors and, as consequence, an increase of the leakage current which is a source of detector noise and heat generation. Such leakage current decreases exponentially with the inverse of temperature and therefore the CMS tracker must operate under the condition that the warmest point on the surface of each silicon sensor is below $-10\ ^{\circ}$C. For this reason, all tracker sub-detectors are cooled by circulating fluids at a temperature between $-20\ ^{\circ}$C and $-25\ ^{\circ}$C.

To avoid condensation of water and growth of ice, which can inflict major damage at such low temperatures, the whole tracking volume needs to be kept sealed and dry. The humidity level has to be controlled by blowing in large quantities of dry gas to force out the water vapor. However, a distributed thermal and hygrometric monitoring of the environmental air is required in the external area surrounding the tracker where cold services are distributed in complex geometries and a safe control of the environmental parameters is more difficult.

For all these reasons, monitoring the ambient parameters, notably temperature and humidity, is crucial in such complex environment, in order to prevent the possible damage of the detector and its expensive service infrastructures. In addition, each tracking detector needs to be as much as possible transparent to particles. This requires the minimization of the mass of all the devices to be installed in situ, together with requirements in terms of radiation resistance to doses ranging from 10 kGy to 1 MGy and insensitivity to magnetic field. In addition, the tracking volume is essentially inaccessible once the detector is installed, therefore frequent recalibrations of the sensors would be impractical.

The experience deriving from the design and production of the first generation of tracking detectors has clearly shown the lack of miniaturized sensors well-suited for local distributed monitoring of the humidity conditions inside harsh and inaccessible environments. In fact, almost all miniaturized humidity sensors commercially available at present for distributed sensing are capacitive (i.e., based on the variation of dielectric constant induced by humidity in a thin polymer layer). In some rare cases, resistive sensors are in use, in particular for high temperature applications. All of these sensors are multi-wired and this makes the remote powering and read-out undesirably complex and space consuming. Furthermore, the electrical sensors suffer from inherent limitations such as transmission loss and susceptibility to electromagnetic interferences, they are not radiation tolerant and only a few ones exhibit a level of accuracy below $\pm 3\%$ RH [1].

On the contrary, fiber optic sensors (FOSs) seem to have the potential to provide a perfectly suited solution to the problem of relative humidity (RH) sensing inside the trackers of the LHC experiments. Indeed, modern fabrication technologies allow obtaining fibers tolerating high radiation levels [2]. This aspect, together with the undeniable advantages of fiber optic technology in terms of reduced size and weight, multiparametric sensing, immunity to electromagnetic interference and water, and corrosion resistance, has promoted renewed interest in the application of FOSs in high radiation environments. Numerous FOSs have been proposed for humidity detection over the years. An extensive review concerning the use of optical sensors for humidity monitoring has been reported by Yeo *et al.* [3].

Since 2011, our research group has been involved in the development of advanced fiber optic RH sensors in collaboration with CERN. The research was firstly focused on the development of radiation tolerant Fiber Bragg Grating (FBG) sensors coated with micrometer-thick polyimide overlays [4], [5]. Collected results provided a clear proof that this innovative technology is a robust alternative to currently used commercial hygrometers. In the meanwhile, due to some limitations of coated FBG-based devices, we also moved towards the development of a second generation of humidity sensors based on Long Period Grating (LPG) coated by a few hundreds of nanometer-thick metal-oxides overlays.

In this paper, we review the results obtained since 2011, during deep experimental campaigns carried out in the CERN laboratories, showing the limits and benefits of both FBG and LPG technologies in light of their application for humidity monitoring in high radiation environments.

2. Optical Fiber Gratings as Relative Humidity Sensors

Fiber gratings consist of a periodic perturbation of the refractive index in the core of the optical fiber and fall in two general classifications based on the period of the grating (typically submicron for FBGs and from 100 μm to 1 mm for LPGs).

In the next sections we explain how it is possible to use the two kinds of gratings as RH sensors and provide the experimental results obtained by using both of them as technological platforms for RH monitoring in HEP environments.

2.1. Fiber Bragg Gratings as Relative Humidity Sensors

A FBG behaves as a wavelength selective filter which reflects light signals at a specific wavelength, named the Bragg wavelength (λ_B), which depends on the fiber effective refractive index (n_{eff}) and the grating pitch (Λ)

$$\lambda_B = 2n_{eff}\Lambda. \tag{1}$$

Both n_{eff} and Λ can be affected by strain and temperature thus making FBGs very popular in temperature and strain sensing applications [6], [8]. In fact, an axial strain in the grating changes the grating spatial period, as well as the effective refractive index and results in a shift of the Bragg wavelength due to the elastic behavior and elasto-optic effect. Moreover, the change of the ambient temperature induces a similar effect, due to the thermal expansion and the thermo-optic effect. Consequently, the Bragg wavelength shift ($\Delta\lambda_B$) due to change in strain (ε) and thermal effect (ΔT) can be expressed as [9]

$$\Delta\lambda_B/\lambda_B = (1 - P_\varepsilon)\varepsilon + [(1 - P_\varepsilon)\alpha + \zeta]\Delta T \tag{2}$$

where P_e is the photo elastic-constant, and α and ζ are the thermal-expansion and thermo-optic coefficients, respectively.

Bare silica fibers are insensitive to humidity. However, it is possible to develop FBG humidity sensors by coating the grating with a hygroscopic material that swells upon water molecules adsorption. The swelling of the moisture sensitive coating strains the fiber, thus inducing mechanical strain to the grating, which results in a Bragg wavelength shift [9], [10]. As a consequence, the adhesion of the coating onto the grating is a crucial aspect which may affect the sensors' performances.

We selected polyimide (PI) as hygroscopic polymeric material for the development of FBG-based RH sensors. Indeed, although its swelling capability is not so high in comparison with other polymers, polyimide exhibits a linear volume expansion when exposed to humidity changes [4].

In presence of ΔRH and ΔT, in the linear assumption, $\Delta\lambda_B$ can be expressed as [4], [9], [10]

$$\Delta\lambda_B = S_{RH}\Delta RH + S_T\Delta \tag{3}$$

where S_{RH} and S_T are the relative humidity and temperature sensitivities of the FBG sensor, respectively.

In the most general case, S_{RH} and S_T are functions of both temperature and humidity [4].

The typical value of S_T is about 10 pm/°C while previous studies demonstrated that the S_{RH} for a 10 μm PI-coated FBG is at best about 1.0 $\div$ 1.5 pm %RH [4]. This means that a very precise temperature compensation scheme is required to decouple the cross-sensitivity to temperature in order to avoid large errors induced on the RH reading. For example, a temperature

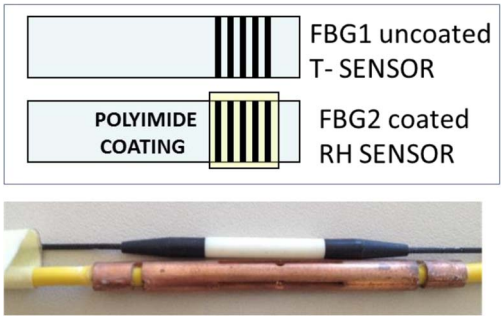

Fig. 1. FOS thermo-hygrometers based on FBG technology developed for the CMS experiment at CERN.

reading error of ± 1 °C corresponds to an error of $7 \div 10\%$ RH in the humidity reading if no compensation is applied.

The solution proposed to CMS and currently in use in the experiment is represented by an optical thermo-hygrometer made of two coupled FBGs: one coated with a micrometer-thick polyimide overlay and another bare, for RH and T readings, respectively, as shown in Fig. 1.

2.2. Long Period Gratings as Relative Humidity Sensors

LPGs are photonic devices allowing the power transfer from the fundamental guided core mode to a discrete number of forward propagating cladding modes and to each of them at a distinct wavelength where the so-called phase matching condition is satisfied:

$$\lambda_{res,0i} = \left(n_{eff,co} - n_{eff,cl}^{0i}\right)\Lambda \tag{4}$$

where $n_{eff,co}$ and $n_{eff,cl}^{0i}$ are the core and i^{th} cladding mode effective indices, respectively, and Λ is the grating period.

As a result of this process (referred to as mode coupling), the LPG transmission spectrum shows several attenuation bands or dips related to the different excited optical fields: the cladding modes. A portion of the electromagnetic field of the cladding modes penetrates into the surrounding medium in the form of evanescent wave, thus making $n_{eff,cl}^{0i}$ (and consequently $\lambda_{res,0i}$) sensitive to the chemical and physical properties of the surrounding environment. Among the different parameters able to influence the spectral features of LPGs, the surrounding refractive index (SRI) sensitivity can be considered as a key feature enabling the use of this kind of sensors in chemical and biological sensing applications through the integration of functional overlays [11], [12].

Moreover, the SRI sensitivity can be optimized for a specific application, by acting on the thickness and optical properties of the functional overlay [13]. Several kinds of materials have been explored as coating for the development of LPG-based RH sensors, including polymers [13], [14], hydrogels [15], gelatine [16], cobalt chloride based materials [17], and SiO_2 nanospheres [18].

In all these cases, the water absorption/desorption in the hygrosensitive coating modifies its RI and thickness, thus creating a spectral variation and amplitude change in the LPG attenuation band, independently from the adhesion properties of the coating onto the grating itself. Accordingly, in presence of relative humidity changes (ΔRH), at constant T and SRI, the resonance wavelength variation for i^{th} cladding mode ($\Delta\lambda_{res,0i}$) can be expressed as follows:

$$\Delta\lambda_{res,0i} = f(\Delta RH) = g\left(\Delta n_{eff,cl}^{0i}\right) \tag{5}$$

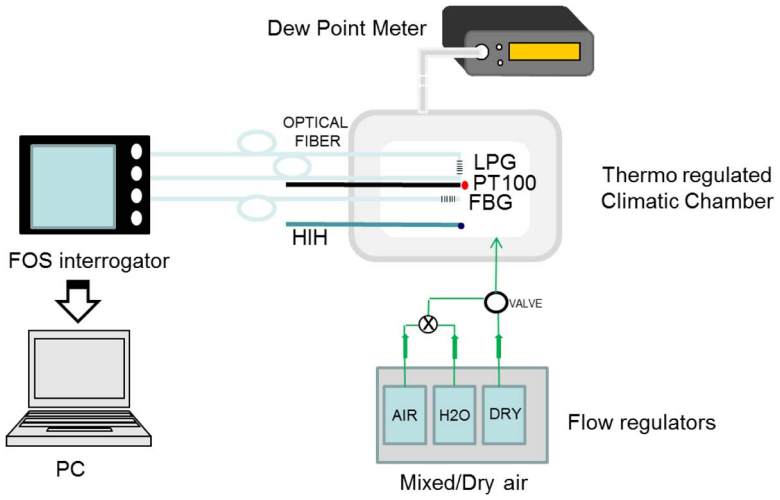

Fig. 2. Experimental set-up used for the tests of the optical sensors based on FBG and LPG technology.

with f and g being typically non-linear functions, generally depending on T and RH. Furthermore, the variations of the refractive index of the cladding related to the i^{th} mode may be expressed as:

$$\Delta n_{eff,cl}^{0i} = h(\Delta n_{co}, \Delta x) \tag{6}$$

where Δn_{co} and Δx_{co} are the variations of refractive index and thickness of the sensitive layer promoted by its water molecules adsorption.

Here, we report on the possibility to use titanium dioxide (TiO_2) and tin dioxide (SnO_2) as nano-scale coating materials of LPGs for humidity monitoring, due to their high refractive index ($n_{TiO_2} = 1.96$ and $n_{SnO_2} = 1.55$) and hygrosensitive characteristics [21]–[26]. Furthermore, the use of metal-oxide layers is expected to avoid the well-known aging problems, typical of polymeric materials.

We point out that in literature there is no evidence of the characterization of coated LPGs at low humidity values (below 20% RH) and temperatures below 15 °C. Moreover, while the radiation effects have been investigated in case of bare LPGs up to 154 Mrad [19], [20], their influence on the sensing performance of coated LPG seems to be completely unexplored.

3. Experimental Set-Up

Fig. 2 shows the set-up used for the experimental tests of the fiber gratings based sensors in the Physics Department-Detector Technology Group (PH-DT) laboratory at CERN.

A suited climatic chamber for humidity measurements has been designed and fabricated in aluminum. The facility is provided with a thermo-regulation circuit for temperature control and stabilization while a manual control of humidity enables the creation of controlled RH levels. A high performance Chilled Mirror Dew Point Hygrometer was used to measure the reference relative humidity. Four resistance thermometers (RTD) were installed close to the optical sensors to guarantee the homogeneity and stability conditions of the temperature in the chamber, together with commercial electronic hygrometers (Honeywell HIH-4000).

A compact and commercial optical interrogator with a measurement range from 1510 nm to 1590 nm and wavelength resolution of 1 pm, was provided for the acquisition of the FOS readings.

In the next sections we provide the results obtained during extensive experimental campaigns carried out in the PH-DT laboratories at CERN, where the temperature and humidity response of optical sensors based on coated FBGs/LPGs have been fully characterized.

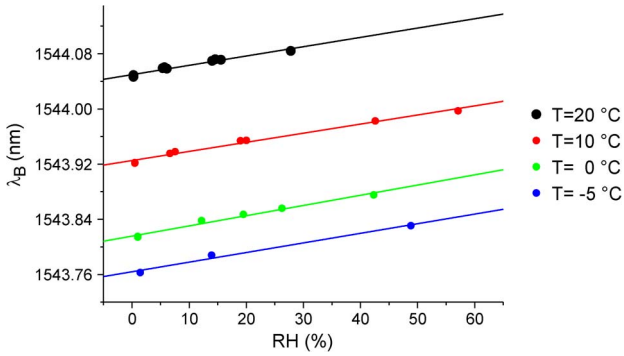

Fig. 3. FBG calibration points at different temperatures.

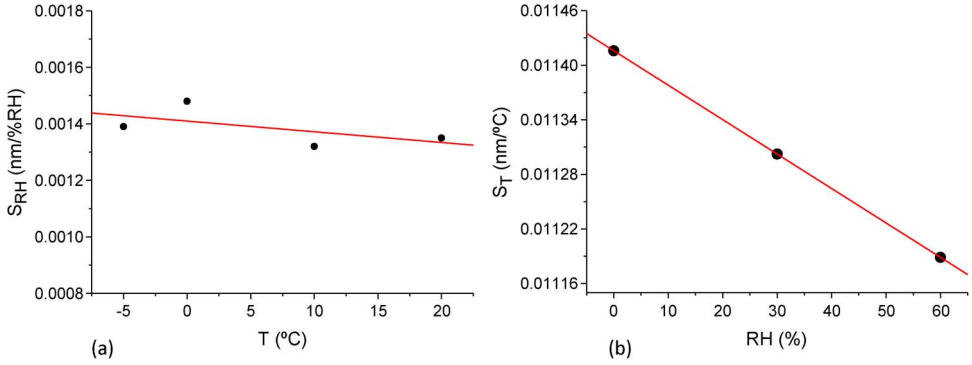

Fig. 4. (a) S_{RH} versus T. (b) S_T versus RH for the selected FBG sensor.

4. Sensing Performances Characterization of FBGs-Based Devices

The FBG sensors selected for the RH measurements were produced under specification with a polyimide coating of 10 μm (± 2 μm) by an external company [4].

RH tests were performed in the range [0–60]% at 4 different temperatures (20, 10, 0, -5 °C), as shown in Fig. 3, where the four RH sensor calibration curves have been reported.

The response of the FBG sensors towards humidity was found to be linear also at temperatures below 0 °C, as emphasized by the fitting curves applied to the data set in Fig. 3. By using these calibration curves, S_{RH} and S_T were evaluated in order to construct the linear model reported in (3).

Slight dependences of S_{RH} on T and of S_T on RH were observed, as shown in Fig. 4(a) and (b). In particular, they both were found to slightly decrease with T and RH, respectively; however mean S_{RH} and S_T values of 1.41 ± 0.07 pm/%RH and 11.40 ± 0.11 pm/°C, respectively, could be evaluated.

A higher order method than that reported in (3) was necessarily introduced to model the above mentioned cross-sensitivity dependencies and the RH was expressed as

$$\mathrm{RH}(\lambda, \mathrm{T}) = \mathrm{p}_{00} + \mathrm{p}_{10}\lambda + \mathrm{p}_{01}\mathrm{T} + {}_{20}\lambda^2 + \mathrm{p}_{11}\lambda\mathrm{T} + \mathrm{p}_{02}\mathrm{T}^2 \tag{7}$$

where $\mathrm{p}_{00} \ldots \mathrm{p}_{02}$ are the fitting parameters. The λT term was used to express the correlation between wavelength and temperature.

Fig. 5 shows the performances of four FBG-RH sensors using this model: the residuals, evaluated as the difference between RH_{FOS} and RH_{ref} are inside ± 2% RH in the steady states.

As to the temperature sensors, commercial FBGs (Micron Optics os4300) were selected. The sensors were fully characterized in the range $[-20, 20]$ °C.

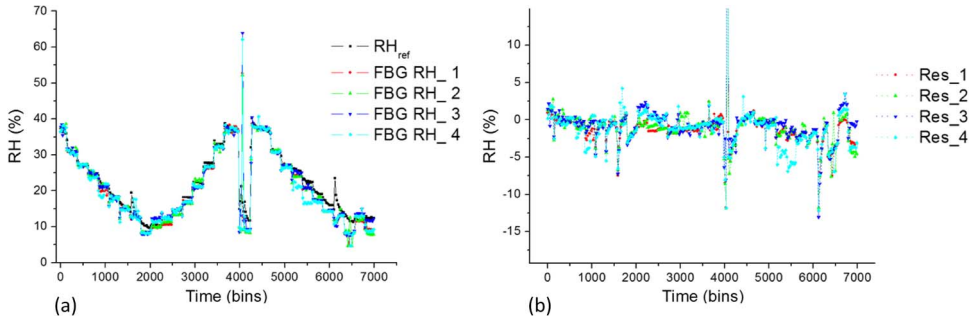

Fig. 5. (a) RH reconstruction from four FBG thermo-hygrometers. (b) Residual (defined as $RH_{FOS} - RH_{ref}$) are $\pm 2\%$ in steady states.

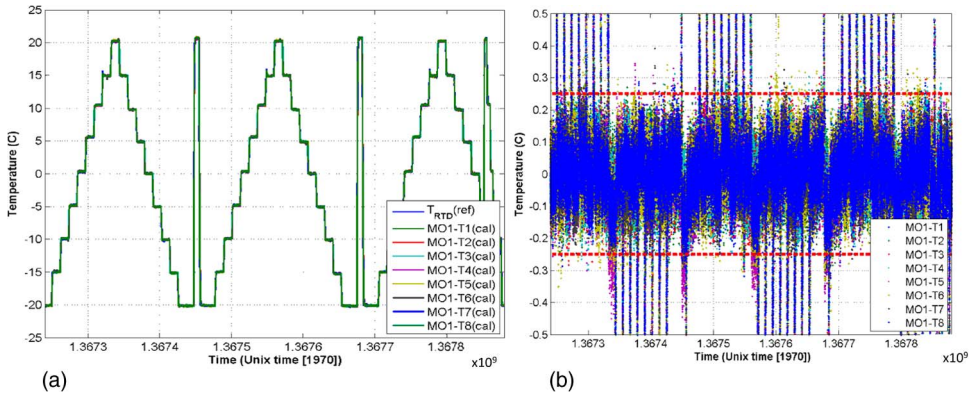

Fig. 6. (a) Temperature reconstruction from 8 FBG sensors. (b) $T_{FOS-Tref}$.

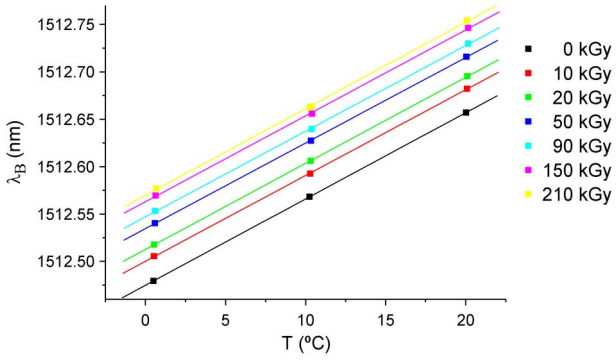

Fig. 7. λ versus T at different doses for the selected FBG- T sensor.

In Fig. 6(a), an example of T reconstruction for 8 optical samples is shown.

Despite the different dynamics of the FOS and the reference sensors, the residuals, defined as the difference between the temperatures measured by the reference sensor and the grating, are inside ± 0.15 °C in steady states, as shown in Fig. 6(b).

The radiation tolerance characteristics of the FBG thermo-hygrometers were also investigated. In particular, incremental irradiation campaigns were performed on samples of RH and T FBG sensors in order to understand the effect of γ-ionizing radiation on their sensing performances.

In Fig. 7, results from one FOS T sample irradiated up to 210 kGy γ-radiation dose are summarized.

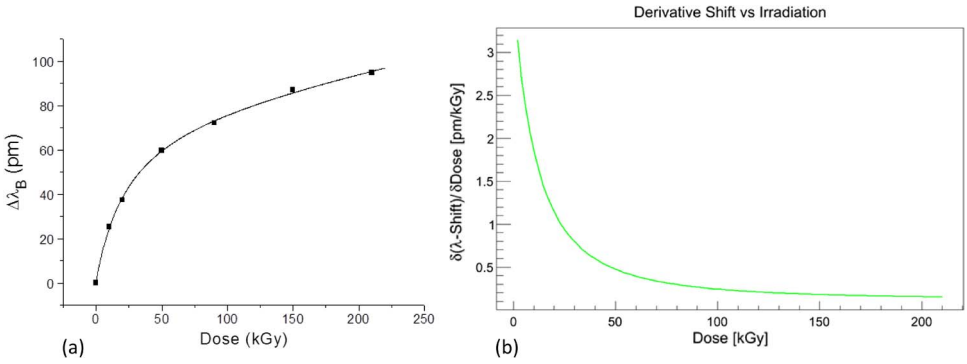

Fig. 8. (a) $\Delta\lambda_B$ versus Dose. (b) $S_{\gamma-rad}$ versus Dose for the selected FBG temperature sensor.

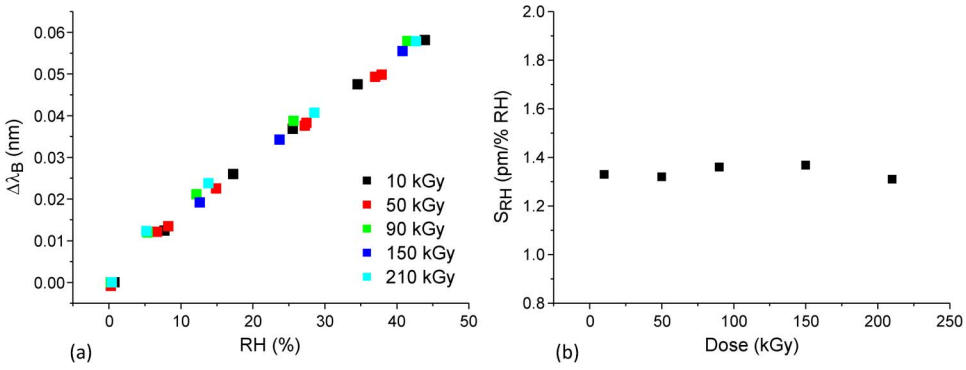

Fig. 9. (a) $\Delta\lambda_B$ versus RH at 20 °C. (b) Invariance of S_{RH} up to 210 kGy for the selected FBG relative humidity sensor.

A radiation-induced red shift was observed after each irradiation step.

The S_T value, evaluated as the slope of the calibration curve at each dose, was found to be unchanged all over the six campaigns. We point out that the wavelength shift is not saturated up to 210 kGy, however, above 100 kGy total adsorbed dose the shift near linearly increases with it, as shown in Fig. 8(a).

Fig. 8(b) shows the sensitivity of the sensor to radiation ($S_{\gamma-rad}$), evaluated as the derivative of the dose induced shift. After a 150 kGy absorbed dose, $S_{\gamma-rad}$ was found to be very low ($\approx$ 0.15 pm/kGy).

This result suggests that the FOS T sensors can be used in high radiation environments just performing a pre-irradiation step at a dose higher than 150 kGy in order to bring them in the "safety zone" where very low $S_{\gamma-rad}$ is guaranteed.

Similar investigations have been performed on FBG-RH sensors. In particular 4 samples have been irradiated up to 210 kGy and results after each campaign demonstrated that the effect of ionizing radiation is negligible on S_{RH} (below the measurement error).

In Fig. 9(a) and (b), results at 20 °C from one sample of FOS RH sensor exposed up to 210 kGy γ-radiation dose are summarized.

Similarly to the T sensors, the RH FBGs also showed a radiation induced wavelength shift.

It is worth emphasizing that, for the exploitation of such FBG-based devices in concrete applications, the use of pre-irradiated sensors (i.e., of coated-FBGs preliminary exposed to doses $>$ 150–200 kGy) helps to decrease the devices sensitivity to further irradiations.

Collected results give a clear demonstration that FBG technology is a robust and valid alternative to currently used electronic humidity sensors in the CMS experiment. For this reason, since December 2013, we have installed 54 thermo hygrometers (72 by the end of summer

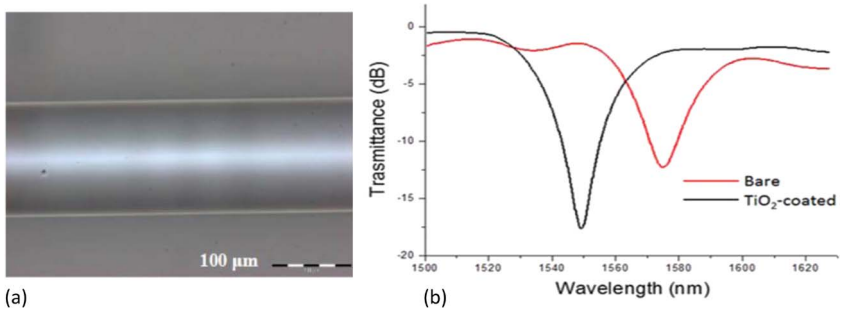

Fig. 10. (a) Microscope image the sample LPG1. (b) Transmitted spectra of bare and coated LPG1.

2014) based on FBG technology for the hygrometric control of the air in critical areas of the experiment where cold services are exposed to condensation.

5. Sensing Performances Characterization of LPGs-Based Devices

LPGs have also been used as advanced technological platforms for the development of a second generation of fiber optic RH sensors. In this case, two different metal oxides, i.e., TiO_2 and SnO_2, have been investigated as sensitive materials due to their good hygroscopic features and high refractive index. In both cases, the sol-gel dip coating method has been selected for their integration (in the form of nano-scale overlays) onto the LPG surface, mainly due to its capability to guarantee a good optical quality, a ring shaped symmetry, and an adequate longitudinal uniformity over the grating length.

Test at different temperatures (including temperatures below 0 °C) in the range [0–70] %RH have been performed in order to identify the best candidate material to use for the development of LPG-based RH sensors.

In the next sections, we provide some details about the fabrication process of TiO_2 and SnO_2 coated LPG sensors and, separately, we present the experimental results obtained during the test campaigns recently carried out at CERN.

5.1. TiO_2 Coated LPG Sensors' Fabrication and Characterization

The deposition procedure used to fabricate TiO_2-coated LPG RH sensors mainly consisted of the sol-gel preparation (using titanium (IV) isopropoxide as titania precursor) followed by a standard dip-coating procedure [12]. More specifically, the fiber was first immersed into the sol-gel solution and then withdrawn with a controlled speed of 100 mm/min in order to allow the formation of a coherent fluid film. The final coating material is typically obtained by a curing step at 150 °C for 10 minutes. Several samples with different TiO_2 thicknesses have been successfully produced.

Here we present results concerning the sample LPG1, characterized by a period $\Lambda = 404$ μm and TiO_2 overlay thickness of $\sim$100 nm.

Fig. 10(a) reports a 20$\times$ optical microscope image of LPG1 after the deposition procedure, from which the smoothness and homogeneity of the deposited layer can be appreciated. The wavelength shift associated to the investigated attenuation band was monitored during all the deposition phases. This guarantees efficient on-line control of the targeted final overlay thickness. Fig. 10(b) shows the transmittance spectra of LPG1, before and after the TiO_2 deposition.

The bare device exhibits an attenuation band (related to the fifth cladding mode) centered at $\lambda_{res,05} = 1589.0$ nm, while the deposition of the TiO_2 layer causes a resonance blue shift of $\sim$24.1 nm together with a $\sim$5 dB increase in its depth. Experimental results provide a first evidence of the optical quality of the deposited overlay, indeed, if an optical lossy overlay is deposited onto the LPG surface, a decrease in the visibility of the attenuation band combined with a spectral broadening would be expected.

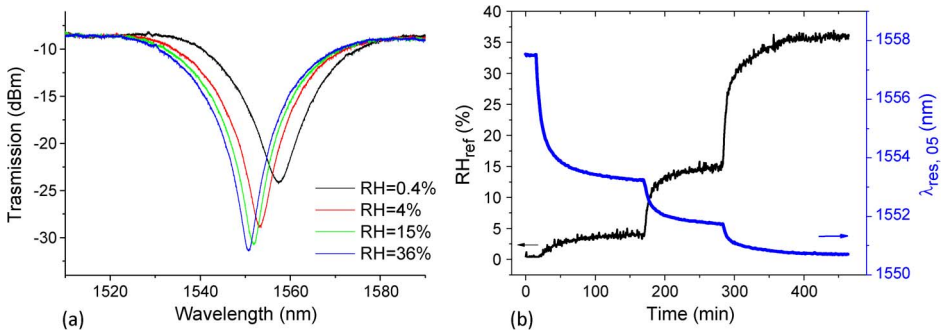

Fig. 11. (a) Transmittance spectra of LPG1 acquired at different RH values. (b) Typical LPG1 response (blue curve) during a RH characterization at 25 °C. The response provided by the reference device is also reported (black curve).

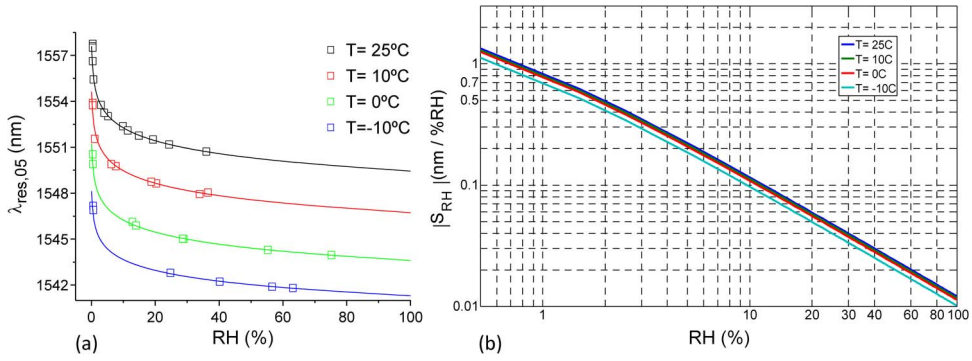

Fig. 12. (a) LPG1 characteristic curves at the four investigated T. (b) SRH as a function of RH.

The performances of LPG1 have been investigated in the range [0–75] %RH, at −10, 0, 10, and 25 °C. Fig. 11(a) shows the LPG1 spectral variations during a characterization test carried out at 25 °C.

As theoretically expected, increasing the humidity content inside the test chamber causes a blue shift of the $\lambda_{res,05}$. This is due to the TiO_2 coating refractive index increase promoted by the higher amount of adsorbed water molecules, which in turn leads to an increase of $\lambda^{05}_{res,cl}$ [22]. Moreover, by increasing the RH value, the attenuation band visibility also increases. This is an important aspect as, in most cases, LPGs coated with "lossy" overlays experience partial or full resonance fading when operating in transition mode [27].

Fig. 11(b) reports the $\lambda_{res,05}$ variations of LPG1 during the same characterization test of Fig. 11(a). For comparison, the response from the reference humidity sensor is also provided. It is worth emphasizing that the response provided by the optical sensor is in agreement with the readings of the reference device. Similar results have also been obtained at 10, 0 and −10 °C, underlying the capability of the device to work properly also at low temperatures in the full RH range of interest.

Fig. 12(a) shows the calibration curves of LPG1 obtained at the four considered temperatures.

In contrast with what observed in case of polyimide-coated FBGs [4], as explained in the previous section, the calibration curves have been found to be non-linear, as a larger $\lambda_{res,05}$ shift was registered at low RH levels. This can also be observed in Fig. 12(b), where the RH sensitivity (S_{RH}) curves of LPG1 versus RH are plotted. At 25 °C, S_{RH} values are between 1.4 and 0.11 nm/% RH in the range [0–10]% RH. It then decreases down to 0.01 nm/%RH at high humidity levels. This sensitivity has to be compared with a uniform S_{RH} in the range $1 \div 1.5\ 10^{-3}$ nm/%RH typical

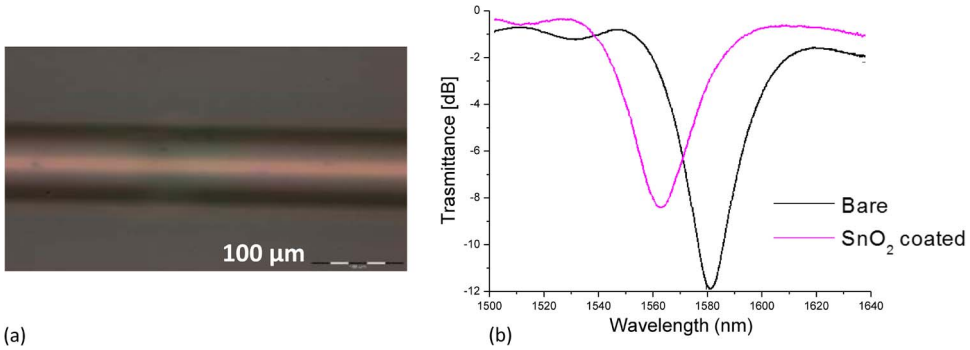

Fig. 13. (a) Microscope image of one of the fabricated SnO_2 sample. (b) Transmitted spectra of bare and coated LPG2.

of polyimide-coated FBG sensors [4]. From Fig. 12(b), a slight dependence of S_{RH} on temperature (a small decrease occurs when temperature decreases) can be also appreciated.

In addition, starting from the characteristic curves reported in Fig. 12(a), working at constant RH, the temperature sensitivity (S_T) of LPG1 can also be retrieved by differentiating the λ-T curves (found to be linear), obtained extrapolating the $\lambda_{res,05}$ values for each temperature from the fitting curves.

As a result, the S_T values (obtained at different humidity levels) were found to slightly decrease with RH; however a mean S_T value of $\sim 0,250 \pm 0.015$ nm/°C has been evaluated in the full RH range.

It is worth noticing that also in case of LPG sensors, a temperature compensation scheme is required in order to reduce the cross sensitivity to unavoidable temperature modifications occurring in real applications. However, in the critical range [0–10] %RH, assuming for the LPG a S_{RHmean} of $\sim$0.5 nm/%RH, a temperature change of 1 °C would induce a 0.5 ÷ 1% RH error if no compensation is applied. This value is significantly better than the thermal cross talk observed in the case of coated FBGs (7–10% RH error for a non-compensated temperature change of 1 °C).

5.2. SnO_2 Coated LPG Sensors' Fabrication and Characterization

SnO_2-coated LPG sensors have also been manufactured through the sol-gel dip coating method: in this case we selected tin (IV) tert-butoxide as tin precursor and used a similar deposition procedure to the one followed for the integration of TiO_2 layers onto the LPGs surface.

Fig. 13(a) reports a typical 20× optical microscope image of a fabricated SnO_2-coated LPG. Also in this case the reported image clearly reveals the smoothness and homogeneity of the deposited layer.

Here we concentrate our attention on the sample named LPG2, characterized by a period $\Lambda = 410$ μm and SnO_2 overlay thickness of $\sim$300 nm.

Fig. 13(b) shows the transmittance spectra of LPG2, before and after the overlay deposition. The bare device exhibits an attenuation band (related to the 5th cladding mode) centered at $\lambda_{res,05} = 1581.5$ nm with a transmitted power of 11.9 dB, while the SnO_2 deposition causes a resonance blue shift of $\sim$18.0 nm together with a $\sim$3.5 dB decrease in its depth.

The sample LPG2 has been characterized at 25 °C in the range [0–50]% RH.

Fig. 14(a) reports the typical spectral variations of LPG2 during an RH characterization test carried out at constant room temperature. Coherently with what observed for LPG1 sample, a blue shift of the $\lambda_{res,05}$ takes place by increasing the level of humidity in the chamber due to the SnO_2 coating refractive index increase promoted by the adsorption of moisture.

Fig. 14(b) reports the $\lambda_{res,05}$ variations (blue curve) of the considered sample during the same test in comparison with the readings of the reference device (black curve). Good agreement

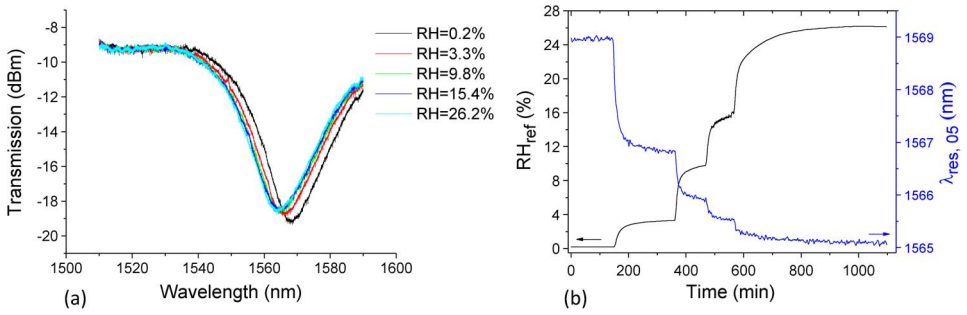

Fig. 14. (a) Transmittance spectra of LPG2 acquired at different RH values during a test at 25 °C. (b) Typical LPG2 response (blue curve) during the same RH characterization at 25 °C.

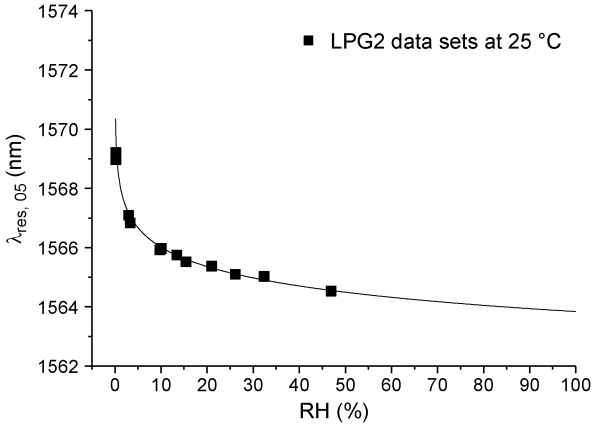

Fig. 15. Calibration curve at 25 °C of the sample LPG2.

with the reference readings can also be appreciated. As already underlined in case of TiO_2 coated LPG based sensor, the LPG2 response toward RH is non-linear, as also emphasized by the calibration curve applied to the data sets at 25 °C shown in Fig. 15.

5.3. Nano-Scale Coated LPG Sensors' Radiation Tolerance Characteristics

In order to identify which one of the two investigated coating materials (TiO_2 and SnO_2) is more suitable for the development of high-performance RH LPG sensors, it is interesting to compare the sensing performances of LPG1 and LPG2 at 25 °C, presented in Sections 5.2 and 5.1, respectively.

In particular, in Fig. 16, we report the calibration curves of the two devices obtained at ambient temperature.

It turned out that the SnO_2-coated sensor experiences lower resonance wavelength shifts upon RH level increase if compared to those presented by LPG1. Indeed, referring to Fig. 16, in the critical operative range [0–10]% RH, the maximum resonance wavelength shifts of TiO_2 coated LPG (black points) resulted to be ∼4 nm while that observed for the SnO_2-coated one (red points) was ∼3 nm. In terms of RH sensitivity, the tin dioxide-based hygrometer showed a S_{RH_mean} ∼0.2 nm/%RH against a value of ∼0.3 nm/RH% obtained with the titania-based counterpart. This behavior is confirmed also at higher humidity values where a smaller sensitivity is obtained compared to that provided by the titania-based probe (e.g., at 40% RH, the SnO_2-coated LPG sensor shows a value of ∼0.02 nm/%RH in comparison of the ∼0.03 nm/RH% shown by the TiO_2-coated device). In addition, the sample LPG1 showed higher saturation thresholds with respect to the LPG2 one.

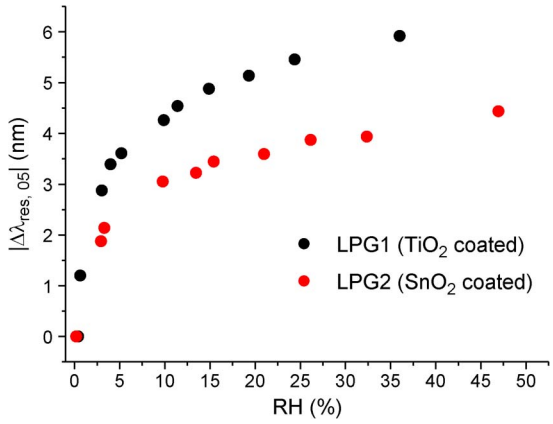

Fig. 16. Comparison between the resonance wavelength shifts induced by incremental changes of the humidity level in the chamber at constant temperature in case of the samples LPG1 (TiO_2 coated) and LPG2 (SnO_2 coated).

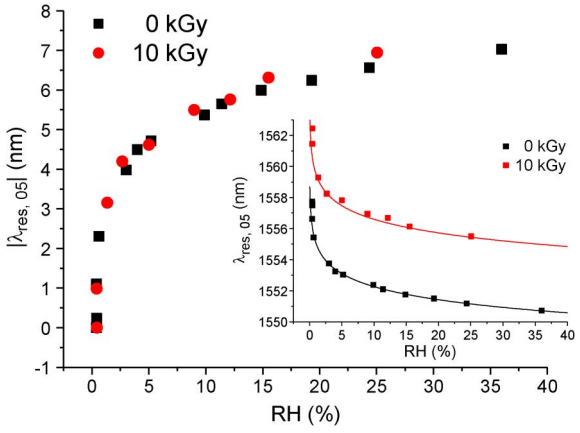

Fig. 17. (a) LPG1 ($\Delta\lambda_{res,05}$, RH) points at 25 °C before (black points) and after (red points) the 10 kGy radiation exposure. Inset: ($\lambda_{res,05}$, RH) points referring to the same tests.

From the collected results, we decided to focus our investigations on the development of TiO_2 coated LPG based sensors and moved on investigating the radiation tolerance characteristics of titania-coated LPGs. Specifically, the radiation effects on TiO_2 coated LPG operation have been investigated by exposing the sample to 10 kGy dose of γ-ionizing radiation. The irradiation process has been performed using a Co^{60} source. Preliminary results evidence a radiation-induced dip wavelength shift of about 4.4 nm in correspondence of 30% RH, as shown in the inset in Fig. 17.

Even if further irradiation campaigns at progressively higher doses are currently in progress in order to confirm these preliminary results, we point out that the observed shift is almost in agreement with radiation hardness investigations conducted on different types of bare LPGs [27].

In particular, the observed shift is of the same order of magnitude of the shift observed with bare chiral LPGs [27] and also similar to that recorded after a dose of 6 kGy with low order modes (8th, 9th, and 10th) in case of a bare turnaround point LPG written in a B/Ge doped fiber [28].

In Fig. 17, the LPG1 $\Delta\lambda_{res,05}$ versus RH at 25 °C, before (black curve) and after (red curve) the irradiation campaign, is depicted. Interestingly, the TiO_2 coated LPG sensor does not lose its excellent capability to respond to RH changes and, apart some variations ($\sim$16%), its characteristic curve still exhibits the same behavior shown before irradiation.

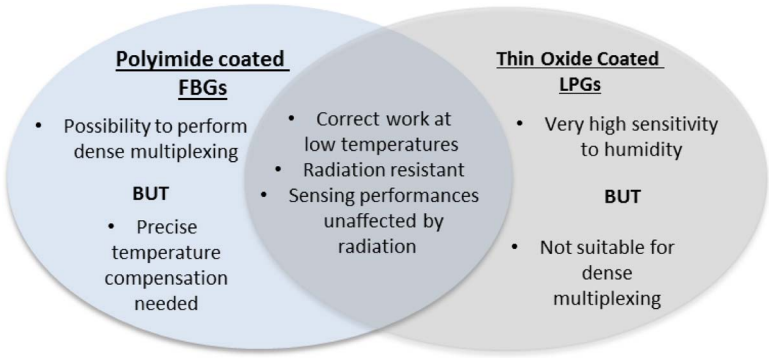

Fig. 18. Main features of polyimide coated FBGs and thin oxide coated LPGs sensors proposed for relative humidity monitoring in high radiation environments.

The obtained results suggest the necessity of taking in account the γ-ionizing radiation effects on the LPG sensor's response in order to fully exploit the extremely sensitivity of these devices HEP applications. We draw attention to the fact that reported data provide the first experimental demonstration of the radiation tolerance of TiO_2-coated LPG sensors for RH monitoring, and envisage good perspectives for an effective exploitation of this technology for RH monitoring in HEP applications.

6. Final Remarks

We first emphasize that our investigations filled the gaps in the state of the art of coated-FBGs/LPGs RH sensors' literature. In particular we demonstrated that both technologies can correctly work at temperature below 0 °C and have good radiation tolerant characteristics. We also point out that there are some aspects which have to be taken into account in order to understand which technology is more or less suitable for specific applications. To this aim, in Fig. 18, we schematically summarize the main features of polyimide-coated FBGs and metal oxide-coated LPG sensors, here proposed for relative humidity monitoring in high radiation environments.

In particular, the choice of using LPGs instead of FBGs-based sensors can be advantageous in some cases, mostly because they are able to provide very high relative humidity sensitivity, especially at very low humidity values. Indeed, as previously discussed, we found that TiO_2-coated LPG sensors show typically S_{RH} values from one to three orders of magnitude higher than that exhibited by FBG-based ones. This is a very relevant feature in many applications, as in case of the CMS experiment, where any humidity sensor is supposed to operate at low humidity as the tracking volume is kept dry in order to avoid water condensation or ice growth. On the other side, compared with FBGs, LPGs are more difficult to be multiplexed mainly due to limitations in terms of available bandwidth. For this reason, in case of applications requesting dense multiplexing, the use of FBG is generally suggested.

7. Conclusion

In this paper, we have reported a comparative study of the properties and performances of two innovative classes of fiber optic sensors for relative humidity monitoring applications in high radiation environments. In particular we have presented our investigations carried out since 2011 in collaboration with CERN in Geneva. The research first focused on the development of relative humidity Fiber Bragg Grating sensors coated with micrometer thin polyimide overlays and recently has been extended to Long Period Gratings. In this last case, two metal oxides (titanium dioxide and tin dioxide) have been tested in order to select the best candidate material to use to coat the LPGs.

We have reported the main steps of our investigations, underlying the limits and benefits of each considered technology. From the experimental test campaigns we found that the TiO_2

coating can guarantee better performances an higher sensitivity to humidity than SnO_2. Moreover we demonstrated the capability of TiO_2-coated LPG sensors to provide very high RH sensitivities (up to 1.4 nm/%RH in correspondence of very low humidity values), which turned out to be from one to three orders of magnitude higher than that exhibited by FBG sensors coated by micrometer thin polyimide overlays. In addition, the sensing performances of LPG-based sensors resulted to be almost unaffected by the exposure to a 1 Mrad dose of γ-ionizing radiation.

Collected results give a clear demonstration that these two technologies represent a robust and valid alternative to polymer-based electronic hygrometers currently used in use in the CMS experiment at CERN, as well as in high-radiation environments.

References

[1] M. Fossa and P. Petagna, "Use and calibration of capacitive RH sensors for hygrometric control of the CMS tracker," 2003, CMS NOTE 2003/24.

[2] A. Cusano, A. Cutolo, and J. Albert, *Fiber Bragg Grating Sensors: Recent Advancements, Industrial Applications and Market Exploitation*, vol. 12. Sharjah, U.A.E.: Bentham, 2011, pp. 218–237.

[3] T. L. Yeo, T. Sun, and K. T. V. Grattan, "Fibre-optic sensor technologies for humidity and moisture measurement," *Sens. Actuators A, Phys.*, vol. 144, no. 2, pp. 280–295, Jun. 2008.

[4] G. Berruti *et al.*, "Radiation hard humidity sensors for high energy physics applications using polyimide-coated fiber Bragg gratings sensors," *Sens. Actuators B, Chem.*, vol. 177, pp. 94–102, Feb. 2013.

[5] A. Makovec *et al.*, "Radiation hard polyimide-coated FBG optical sensors for relative humidity monitoring in the CMS experiment at CERN," *J. Instrum.*, vol. 9, no. 3, p. C03040, Mar. 2014.

[6] K. O. Hill and G. Metlz, "Fiber Bragg grating technology fundamentals and overview," *J. Lightw. Technol.*, vol. 15, no. 8, pp. 1263–1276, Aug. 1997.

[7] Y. J. Rao, "In-fibre Bragg grating sensors," *Meas. Sci. Technol.*, vol. 8, no. 4, pp. 355–375, Apr. 1997.

[8] A. D. Kersey *et al.*, "Fiber grating sensors," *J. Lightw. Technol.*, vol. 15, no. 8, pp. 1442–1463, Aug. 1997.

[9] T. L. Yeo *et al.*, "Characterization of a polymer-coated fiber Bragg grating sensor for relative humidity sensing," *Sens. Actuators B, Chem.*, vol. 110, no. 1, pp. 148–155, Sep. 2005.

[10] P. Kronenberg, P. K. Rastogi, P. Giaccari, and H. G. Limberger, "Relative humidity sensor with optical fiber Bragg grating," *Opt. Lett.*, vol. 27, no. 16, pp. 1385–1387, Aug. 2002.

[11] I. Del Villar, I. Matías, F. Arregui, and P. Lalanne, "Optimization of sensitivity in long period fiber Gratings with overlay deposition," *Opt. Exp.*, vol. 13, no. 1, pp. 56–69, Jan. 2005.

[12] A. Cusano *et al.*, "Mode transition in high refractive index coated long period gratings," *Opt. Exp.*, vol. 14, no. 1, pp. 19–34, Jan. 2006.

[13] T. Venugopalan, T. L. Yeo, T. Sun, and K. T. V. Grattan, "LPG-based PVA coated sensor for relative humidity measurement," *IEEE Sensors J.*, vol. 8, no. 7, pp. 1093–1098, Jul. 2008.

[14] T. Venugopalan, T. Sun, and K. T. V. Grattan, "Long period grating-based humidity sensor for potential structural health monitoring," *Sens. Actuators A, Phys.*, vol. 148, no. 1, pp. 57–62, Nov. 2008.

[15] Y. Liu *et al.*, "Long-period grating relative humidity sensor with hydrogel coating," *IEEE Photon. Technol. Lett.*, vol. 19, no. 12, pp. 880–882, Jun. 2007.

[16] K. M. Tan, C. M. Tay, S. C. Tjin, C. C. Chan, and H. Rahardjo, "High relative humidity measurements using gelatin coated long-period grating sensors," *Sens. Actuators B, Chem.*, vol. 110, no. 2, pp. 335–341, Oct. 2005.

[17] M. Konstantaki, S. Pissadakis, S. Pispas, N. Madamopoulos, and N. A. Vainos, "Optical fiber long-period grating humidity sensor with poly(ethylene oxide)/cobalt chloride coating," *Appl. Opt.*, vol. 45, no. 19, pp. 4567–4571, Jul. 2006.

[18] D. Viegas *et al.*, "A fiber optic humidity sensor based on a long-period fiber grating coated with a thin film of SiO2 nanospheres," *Meas. Sci. Technol.*, vol. 20, no. 3, p. 034002, Mar. 2009.

[19] A. Gusarov and S. K. Hoeffgen, "Radiation effects on fiber gratings," *IEEE Trans. Nucl. Sci.*, vol. 60, no. 3, pp. 2037–2053, Jun. 2013.

[20] S. Kher, S. Chaubey, S. M. Oak, and A. Gusarov, "Measurement of γ-radiation induced refractive index changes in B/Ge doped fiber using LPGs," *IEEE Photon. Technol. Lett.*, vol. 25, no. 21, pp. 2070–2073, Nov. 2013.

[21] E. Davies *et al.*, "Sol-gel derived coating applied to long-period gratings for enhanced refractive index sensing properties," *J. Opt. A, Pure Appl. Opt.*, vol. 11, no. 1, p. 015501, Jan. 2009.

[22] G. Montesperelli *et al.*, "Sol-gel processed TiO_2-based thin films as innovative humiditysensors," *Sens. Actuators B, Chem.*, vol. 25, no. 1–3, pp. 705–709, Apr. 1995.

[23] B. C. Yadav, N. K. Pandey, A. K. Srivastava, and P. Sharma, "Optical humidity sensors based on titania films fabricated by sol–gel and thermal evaporation methods," *Meas. Sci. Technol.*, vol. 18, no. 1, pp. 260–264, Jan. 2007.

[24] M. Consales *et al.*, "Nanoscale TiO_2-coated LPGs as radiation-tolerant humidity sensors for high-energy physics applications," *Opt. Lett.*, vol. 39, no. 14, pp. 4128–4131, Jul. 2014.

[25] M. Consales *et al.*, "Fiber optic humidity sensors for high-energy physics applications at CERN," *Sens. Actuators B, Chem.*, vol. 159, no. 1, pp. 66–74, Nov. 2011.

[26] P. Chatelon, C. Terrier, and J. A. Roger, "Electrical and optical property enhancement in multilayered sol-gel-deposited SnO_2 films," *Semicond. Sci. Technol.*, vol. 14, no. 7, pp. 642–647, Jul. 1999.

[27] I. R. Del Villar, F. J. Matias, and M. Arregui, "Nanodeposition of materials with complex refractive index in long-period fibre grating," *J. Lightw. Technol.*, vol. 23, no. 12, pp. 4192–4199, Dec. 2005.

[28] S. Kher, S. Chaubey, R. Kashyap, and S. M. Oak, "Turnaround-point long-period fiber gratings (TAP-LPGs) as high-radiation-dose sensors," *IEEE Photon. Technol. Lett.*, vol. 24, no. 9, pp. 742–744, May 2012.